

**Proceedings
of the International Symposium on
Aerospace and Fluid Science**

in commemoration of the 50th anniversary of
Institute of Fluid Science

Sendai Memorial Hall, Sendai, Japan
November 14-16, 1993

Institute of Fluid Science
Tohoku University

Contents

Plenary Lectures

Boiling Heat Transfer in Microgravity J. Straub, M. Zell and B. Vogel	3
Theoretical Microgravity Fluidynamics H. F. Bauer	30
Summary of Adaptive Structures at Jet Propulsion Laboratory B. K. Wada and A. Garba	50
Transitional Regime Aerodynamics and Real Gas Effects M. S. Ivanov	77

Hypersonic Flow and Propulsion

Effects of Leading Edge Bluntness on Control Flap Effectiveness at Hypersonic Speeds J. L. Stollery and D. Kumar	105
Hypersonic Studies for ESA in the Aachen Shock Tunnel TH2 H. Grönig	111
Hypersonic Research Activity in Marseille R. Brun	121
Scramjet Research Activities at the NAL Kakuda Research Center H. Miyajima	123
Shock Tube Studies of Strong Shock Waves H. Honma	128
Thermochemical Nonequilibrium Flow Analysis in Atmospheric Entry Conditions Y. Sakamura and M. Nishida	149

Boiling Heat Transfer in Microgravity

J. Straub, M. Zell and B. Vogel

Laboratory for Applied Thermodynamics and
Technology under Microgravity
LATTUM
Technical University Munich, Germany

Summary

Experimental investigations of saturated and subcooled pool boiling have been conducted under microgravity to get improved understanding of the gravity effects on pool boiling phenomena and heat transfer. Additional parameter studies in pool boiling by variation of fluid state and heater geometries in combination with gravity variance yield a new understanding of thermo- and fluiddynamic phenomena, which are involved in the global heat transfer process „boiling“. Experimental results give improved knowledge of fundamentals in boiling heat and mass transfer and demonstrate the applicability and high efficiency of nucleate pool boiling for heat exchange facilities also for upcoming space stations or -platforms.

This report is concerned with the present state of the art on boiling under microgravity at the various modes of heat transfer as nucleate boiling, critical heat flux and film boiling. The microgravity results are compared to data obtained under the same conditions with earth gravity.

The mechanisms of heat transport are discussed and comments are made in respect to further experimental and theoretical studies under microgravity for a better understanding of the complex boiling process.

Keywords: pool boiling, microgravity, heat transfer, evaporation, condensation, critical heat flux, film boiling, boiling mechanism, micro-wedge model

1. Introduction and Objectives

Since the first boiling curve obtained by Nukiyama in 1934 [1], many investigations on boiling and two-phase flow heat transfer have been performed in the past sixty years. Nevertheless, the interest in boiling heat transfer is growing continually, documented by the numerous publications that appear in journals and conference proceedings. Dhir [2] quoted two reasons for this increasing interest in his keynote presentation at the 9th International Heat Transfer Conference, Jerusalem, 1990:

1. Boiling is a very efficient mode of heat transfer and as such is employed in component cooling and in various energy conversion systems. The quest for improvement in the performance of the equipment and the demand imposed by new high density energy systems continue to motivate studies on boiling heat transfer.
2. Boiling is a extremely complex and illusive process, which continues to baffle and challenge inquisitive minds.

We continue with Dhir's comment:

Unfortunately, for a variety of reasons, fewer studies have focused on the physics of the boiling process than have been tailored to fit the needs of engineering endeavors. As a result, the literature has been flooded with correlations involving several adjustable parameters. These correlations can provide quick input to design/performance/safety issues and hence are attractive on a short-term basis. However, the usefulness of the correlations diminishes very rapidly as parameters of interest start to fall outside the range of physical parameters, for which the correlations are developed. Also, correlations involving several empirical constants tend to cloud the physics. Thus, if we wish to reduce the repetition of experimental effort in response to changes in the physical parameters of interest in an engineering enterprise, it is important to place greater emphasis on fundamental understanding of this process. A persistent effort in this direction will go a long way in transforming studies of boiling heat transfer from an art to a science and would be attractive and exciting to new researchers.

We fully agree with this statement, and our experience in studying the effect of gravity as a variable parameter results in the same: "the usefulness of the correlations diminishes very rapidly" outside the range of earth gravity. This result may indicate that the physics of the boiling process is indeed not properly understood and is poorly represented in most correlations, if they are extrapolated to lower or higher acceleration values than earth gravity can provide.

The boiling process is very complex owing to the interaction of numerous factors and effects, as the interaction between the solid surface of the heater with the liquid and vapor, interaction between liquid and vapor itself, and the transport of liquid and vapor. Thus the microgravity environment offers the unique opportunity to study these interaction processes without, or at least with reduced buoyancy forces. Larger bubbles are generated so that optical observations can be employed to study the fundamental basis of boiling.

Thus, the basic objectives of the studies about boiling heat transfer under microgravity can be summarized in answering the following questions:

- Is boiling a stable process in a low gravity environment?
- Can the process be used for space applications?
- Can the high heat transfer coefficients be maintained and how are they compared to terrestrial values?
- What is the role of buoyancy and the departure diameter of bubbles in boiling?

- What are the dominating mechanisms, which determine the heat transfer?
- Can the correlations developed for boiling heat transfer on earth be extrapolated for applications in low gravity?
- Are these correlations physically well based?

2. Boiling technology

A heat transfer process between a solid surface, heated or cooled, and a fluid is generally described by Newton's law:

$$\dot{Q} = \alpha \cdot A \cdot (T_w - T_\infty) \quad (1)$$

Where \dot{Q} is the transferred heat flux, α is called the heat transfer coefficient, A is the area involved in the heat transfer, T_w is the surface temperature of the solid wall, and T_∞ is the bulk fluid temperature in some distance from the wall. If a certain heat flux \dot{Q} is transferred in technological processes, the area A and the temperature difference $(T_w - T_\infty)$ should be as small as possible; the first one for a smaller design of the heat exchanger and for the reduction of material and investment costs, and the second for higher efficiency of the thermal process. As a result, the heat transfer coefficient α should be as high as possible. Boiling heat transfer coefficients are some orders of magnitude higher than those in single phase flows. Therefore, the boiling process has a great technological significance.

The heat transfer coefficient in boiling is a complex function combining many different interacting parameters. Therefore, the usual manner to describe transport problems in fluid motion by solving the partial differential equations of the conservation laws can not be applied. Boiling heat transfer correlations are therefore based on optical observations and experimental data and can generally only be applied within the range of parameters, for which they are developed. For more general application in heat transfer, dimensionless parameters such as Nu-, Re-, Ra- and Fo-numbers were often formed to make the correlations independent from the applied scale. As a characteristic length scale in boiling, the Laplace coefficient L or the departure diameter D of the bubble, according to Fritz [3], is used most frequently, written with variable system acceleration a/g :

$$D = C \cdot L(a/g)^{-1/2} \quad \text{with} \quad L = \left(\frac{\sigma}{g(\varrho_l - \varrho_g)} \right)^{1/2} \quad (2)$$

where σ is the surface tension, ϱ_l and ϱ_g are the densities of the liquid (index l) and vapor (index g), C is a factor related to the wetting angle between the solid surface and the liquid, g the earth gravity and a the actual system acceleration.

Thus it is evident that even in empirical correlations the actual acceleration is an important factor. Up to the present, no efforts have been made to verify experimentally how

the influence of gravity can be correctly modelled in the boiling correlation. Therefore, as it will be shown later, it is not surprising that the existing correlations are quite contradictory in their representation of the influence of gravity.

3. Earlier low gravity studies

In the 1960s, an interest in the performance of boiling in gravity fields other than earth gravity arose in the United States in regard to the design of heat transfer devices for space vehicle applications. As a result, various studies have been initiated to examine both reduced and enhanced gravity effects. The influence of reduced gravity was studied in drop towers with experiment times less than 1 second. Therefore, these results are not be regarded to be representative for steady state conditions. Furthermore, the results have not been unambiguous, nevertheless, it is regrettable that they are not adequately recognized in the literature of boiling heat transfer. Unfortunately, these first studies came to an end with a change of interest in the US space program at the end of the 1960s.

A review of these earlier studies of approximately 25 papers and reports is researched by Siegel [4], especially for cryogenic fluids by Clark [5], for Soviet research by Verkin and Kirichenko [6] and a resume of his own studies during the 1960s and 1970s is recently presented by Merte [7]. Our own research of the last ten years is published in : Weinzierl [8], Zell [9], Weinzierl [10], Weinzierl [11], Straub [12], Zell [13], Straub [14], Zell [15], Straub [16] and Vogel [17]. Results from new experiments conducted in various facilities are reported from our US and Japanese colleagues Ervin et al. [18] and Oka et al. [19].

4. Facilities used to compensate earth gravity

The earth gravity force on a body can be compensated either by acceleration in free fall, or by centrifugal force in direct opposition to the gravity force. The first category includes all "free fall" systems like: drop towers, parabolic trajectories of aircraft or ballistic rockets. The second category includes all space systems flying in an orbit around the earth.

In preparation of a shuttle flight for the GAS (Get Away Special) program, scheduled first in 1986, we began to study boiling on wires and flat plates with TEXUS 3 in 1980. It is known that the microgravity environment is as good as $a/g < 10^{-4}$ and the experimental time is 6 minutes. Even TEXUS flights are not so numerous as to study all parameters and modes of boiling heat transfer, therefore we strengthened our boiling program with several campaigns of parabolic aircraft flights KC 135 at the Johnson Space Center in Houston in 1985. During the parabolic trajectory low gravity of about $a/g = \pm 0.03$ over a period of 20 sec can be obtained, followed by a high gravity period with $a/g = 1.8$. Thus in one sequence, a variation from low to high gravity can be researched and a direct comparison between low and high gravity results is possible

under the same experimental conditions. During a one day flight, a series of 30 parabolas are flown. In these parabolic flights, the experimenter can use laboratory hardware, and handles the hard- and software himself, thus insuring the complete experiment control and optimal scientific results.

5. Instrumentation

For TEXUS and parabolic flights different cells with similar design were used as shown in Fig 1. The experimental cell was completely filled with liquid and a metal bellows compensated the volume change during boiling and kept the pressure constant according to the counterpressure on the opposite side of the bellows. Thus, by control of the counterpressure with compressed air, the liquid state could be changed from saturation to subcooled at a constant liquid bulk temperature.

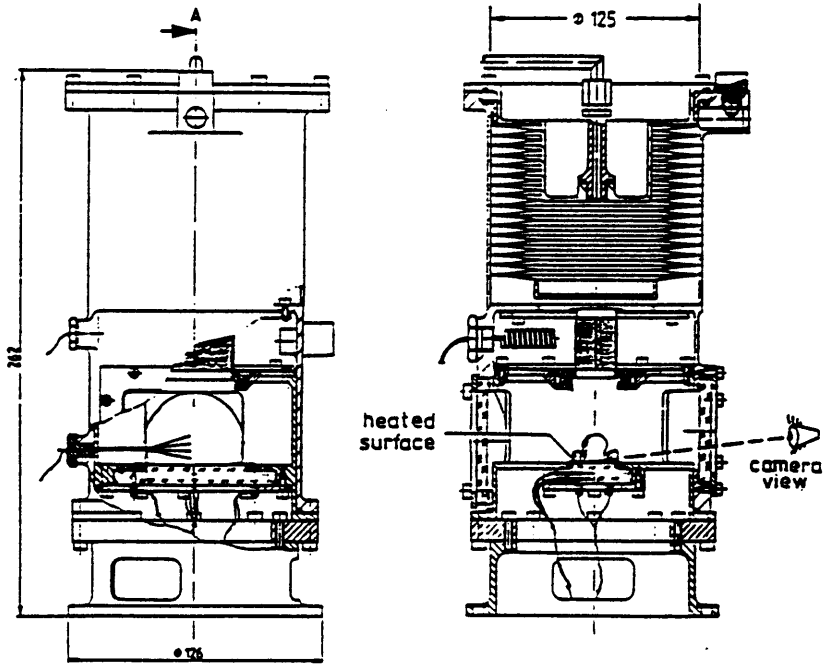


Fig. 1 Experimental cell for TEXUS. For KC 135, a similar design for higher pressure up to 45 bar was used with a larger volume of 2 ltr. The volume compensation was done in a separate cell by a bellows.

While in the TEXUS cell one heater was used at a time (wire or plate), three different heaters were simultaneously installed in the cell for KC 135 and studied one after each other (platinum wire with diameter of 0.05 and 0.2 mm and 50 mm length, a gold

coated flat plate $40 \times 20 \text{ mm}^2$ and in some flights a gold coated glass tube with a diameter of 8 mm and 50 mm length instead of one wire). The platinum wires and the gold coatings are simultaneously used as resistance heater and resistance thermometer, measuring heat flux levels and average heater temperatures using voltage and current. The bulk liquid state is measured by several thermocouples and pressure transducer. The cell temperature can be controlled up to $110 \text{ }^\circ\text{C}$.

Optical recording was possible through glass windows in the pressure cell by a 16 mm Teledyn film camera with 18 and 100 fps in TEXUS, and by a Arriflex camera synchronized with a stroboscope flash in the parabolic flight set-up.

In the TEXUS arrangement, the experiment was controlled by a timer module in the electronics and the data were transmitted to the ground by telemetry. In the aircraft, modified laboratory hardware and standard commercial equipment were used like: power supplies, digital voltmeter, scanner and a personal computer to control the experiment and record the data. The gravity level was determined by a 3-axis accelerometer. Due to the low maximum pressure of 2 bar of the TEXUS cell, R 113 was studied here at a bulk liquid temperature of about $26 \text{ }^\circ\text{C}$ and a reduced pressure $p/p_c = 0.013$. To cover a wide range of pressure from $p/p_c = 0.11$ to 0.7 , the refrigerant R 12 was used as test fluid in the aircraft flights (p/p_c is the reduced pressure, p the saturation pressure and p_c the critical pressure). The bulk temperature and pressure of the liquid were kept constant and at each parabola only one heater was in operation. After completing one boiling curve with 6 to 8 heat flux levels, one of the other heaters was used at the same fluid state. By changing the bulk pressure, we investigated 7 saturated and 26 subcooled fluid states.

6. Gravity as a parameter in the heat transfer correlations

All correlations for boiling heat transfer are based on physical mechanisms or developed empirically under the conditions of earth gravity; gravity is therefore used as a constant factor and is not considered as a parameter. However, if buoyancy is directly used in the physical models as the driving force for heat transfer, or if the "departure diameter" of the bubbles is introduced in empirical relations, then gravity is raised to a significant physical parameter. A comparison of those relations, extrapolated to lower or higher gravity levels, with experimental data will give a significant indication concerning the interpretation of the physical mechanisms of boiling, and of the correct modelling of the dominating effects. If we assume that gravity is a parameter and that all other parameters are constant, we can analyze the correlation in respect to the effect of gravity, which can be expressed in a power law as:

$$\alpha/\alpha_1 = (a/g)^n \quad (3)$$

where α/α_1 is the ratio of the heat transfer coefficients, with α_1 the value at earth

gravity g and a/g is the fraction of the acceleration change. The sign and the value of the exponent n indicates the change of the heat transfer ratio.

The numerous correlation developed for nucleate pool boiling will not be discussed in detail in the framework of this paper. Briefly stated, they can be classified in 3 categories:

- 1. physically based equations (saturated fluid state $n = 1/2$, subcooled $n = 0$),
- 2. dimensionless group correlations ($-0.35 < n < 0.5$),
- 3. empirical relations.

For the process of nucleate boiling the physically based equations are supported by the following observations: after a bubble is formed in the superheated liquid layer by activation of a nucleate site, the bubble grows by evaporation in the superheated liquid boundary layer. The bubble departs from the surface, when a size is reached, at which the upward forces exceed the adhesive forces. During the departure, a part of the superheated boundary layer follows in the wake as drift flow, transporting the bubbles' enthalpy and superheated liquid into the cooler liquid bulk, while cold liquid flows back into the cavity and is heated by transient heat conduction. At lower heat fluxes, when bubbles do not occupy the entire surface, free convection can also contribute to the heat transfer. Normally, under upward heating conditions, the mean upward force is the buoyancy force, and even drift and free convection flow depend on buoyancy.

7 Nucleate boiling

7.1 Results from aircraft flights

Saturated fluid state, $0.1 < p/p_c < 0.7$

During a typical parabola sequence of nucleate boiling, Fig 2, the gravity level a/g , the temperature difference $\Delta T_{sat} = T_w - T_{sat}$ and the power \dot{q}_w of the heater are recorded versus the experimental time. The power was switched on allways during the low gravity period, thus eliminating natural convection. Due to the small heat capacity of the heater, the temperature response was very fast after power on and after the change of power at 45 sec. At a constant power level from 45 to 94 sec the temperature remains constant even when the acceleration increases from $a/g \approx 0.01$ to 1.8 and decreases to 1 again. The small wiggles in the temperature curve are due to the last digit in the resolution of the temperature. The photographs show the dependence of bubble size on gravity, large bubbles at low gravity and small bubbles at high gravity. Between $a/g = 1.8$ and 1 the average bubble size is barely reduced. It is clearly demonstrated that the heat transfer coefficient is neither influenced by gravity nor by the bubble size at this fluid state. α/α_1 remains nearly constant, but even ratios of $\alpha/\alpha_1 > 1$ have been observed at lower heat flux levels.

These investigations are carried out for saturated and subcooled fluid states from $0.1 < p/p_c < 0.7$ and for four heater configurations: wires with 0.05 mm dia. and 0.2 mm dia., flat plate gold coated surface 40 x 20 mm² and tube 8 mm dia. and 50 mm length.

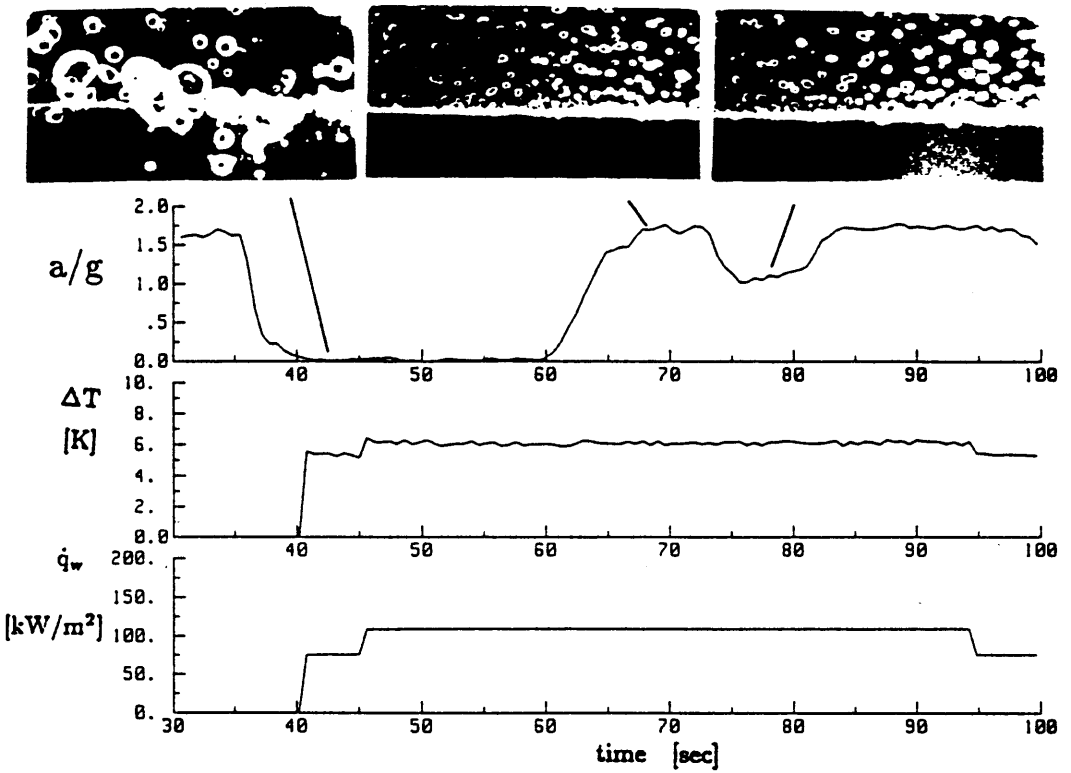


Fig. 2 A parabola sequence, a/g level, wire super heat temperature $\Delta T = T_w - T_{sat}$, heat flux at nucleate boiling $p/p_c = 0.18$, versus time

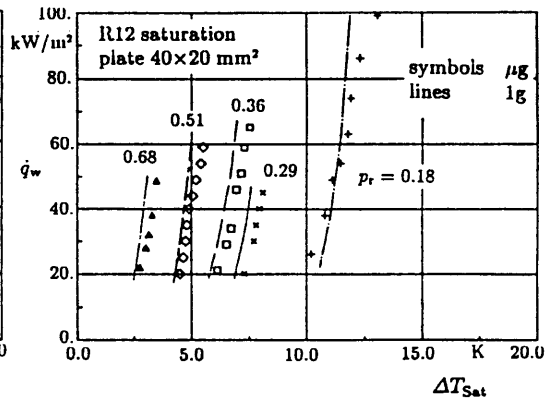
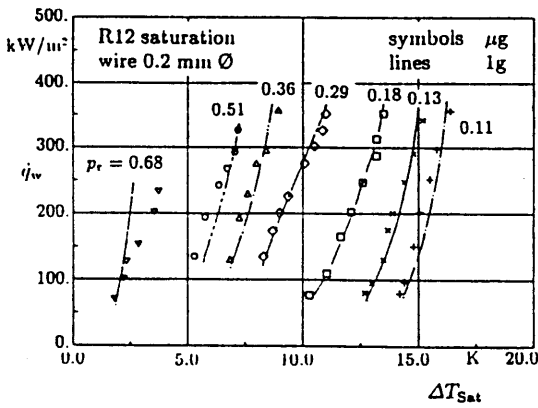


Fig 3: wire 0.2 mm dia.

Fig 4: flat plate 40 x 20 mm

Nucleate boiling curve in R12 at various saturated fluid states

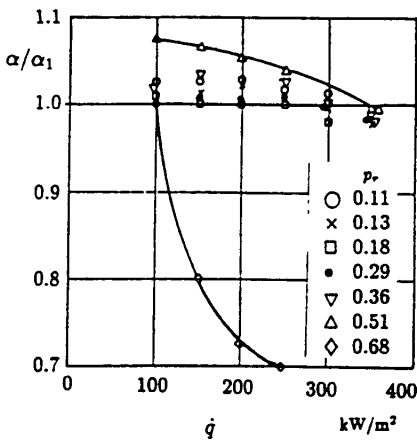


Fig 5: wire 0.2 mm dia.

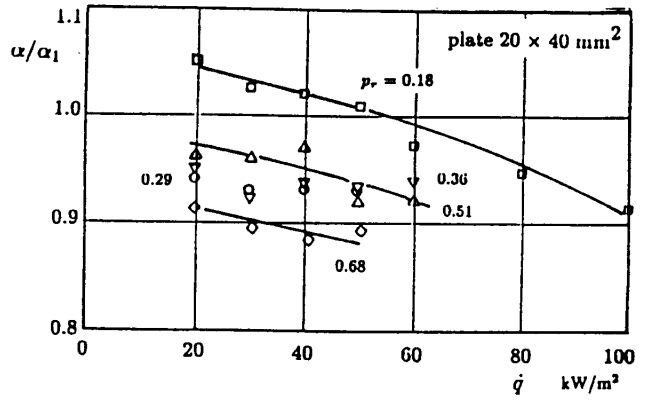


Fig 6: flat plate 40 x 20 mm

Heat transfer ratio according values from Fig 3 and Fig 4

The results are evaluated for all heaters by Zell [15] and plotted as boiling curves with the heat flux density \dot{q}_w versus the temperature difference $\Delta T_{sat} = T_w - T_{sat}$. Only two examples will be shown for the wire 0.2 mm dia. and the flat plate with the bulk liquid being at saturated state for different p/p_c values in Fig 3 and 4. The symbols represent the data obtained at low gravity $a/g = \pm 0.02$, while the lines represent $a/g = 1$ reference data measured immediately after low gravity in the consecutive period of the parabola. The evaluation with respect to the heat transfer ratio α/α_1 versus heat flux density is shown for these two heaters in Fig 5 and 6. From these figures, it can be seen that the heat transfer coefficient for wires is even higher than at earth gravity for low heat flux levels. This may be attributed to the fact that at low gravity all nuclei sites around the wire are equally activated. As a result, boiling occurs symmetrically around the wire at low gravity, whereas at 1 g the lower stagnation point is cooled by free convection and only the upper circumference of the wire is preferred for boiling. Similar behavior can be observed with the other geometries: if convection is eliminated, more nuclei sites are activated at low heat fluxes. The reduction of the heat transfer coefficient at higher heat flux is caused by the larger bubbles and the connected increase of dry areas at the heater below them. At higher system pressure, especially observed on the wires at $p/p_c = 0.68$, α/α_1 decreases to 0.75 with higher heat flux. This may be due to the small surface tension closer to the critical point. We have observed similar behavior on the tube and on the wire with 0.05 mm diameter.

Subcooled fluid states

Many subcooled fluid states have been investigated. The values at low gravity and at 1g are nearly identical. Thus the heat transfer coefficient is nearly independent from gravity even in subcooled nucleate boiling.

7.2 Results from TEXUS flights at low pressure

7.2.1 Boiling on wire

Saturated state

In the TEXUS flights, we have used R 113 as a test fluid with bulk temperature about $T_B = T_{sat} = 26 \text{ }^\circ\text{C}$ with heat fluxes from 40 to 276 kW/m^2 . At low heat fluxes the heat transfer coefficient is the same as in the reference experiment at $1g$ and is about 0.96 at higher heat fluxes. Due to the good quality of the acceleration level $a/g < 10^{-4}$ and no noticeable disturbance in the acceleration, we can observe in the film the following mechanisms:

- single bubbles spring from the surface in all directions
- two or three bubbles coalesce at the wire, and jump from the surface,
- bubbles have various sizes and departure frequencies, the size is two or four times larger than the diameter of the wire,
- the frequency increases with increasing heat flux,
- the bubbles do not condensate, they coalesce in the liquid to larger bubbles,
- convection is induced by the departure of springing bubbles.

Subcooled boiling:

By increasing the pressure to $p = 1 \text{ bar}$ at $26 \text{ }^\circ\text{C}$ bulk temperature, a subcooling of $\Delta T = 22 \text{ K}$ was established. Between 40 and 441 kW/m^2 , steady state nucleate boiling was achieved. At the next step of the heat flux of 450 kW/m^2 film boiling occurred, and the power was switched off by an automatic control system. At the $1g$ reference test, which was influenced by convection, boiling begins at a heat flux of 131 kW/m^2 . The heat transfer coefficient is the same at lower heat fluxes and 0.98 at higher heat fluxes compared to $1g$. We observed the following:

- the bubbles are usually attached to the wire;
- after a lifetime of some tenth of a second they can condense, however, some have a much longer lifetime than at $1g$;
- only a few bubbles depart from the heater surface due to the coalescence process and they condense immediately after departure. At higher heat fluxes, more bubbles depart from the surface, the bubble population density increases as well as the number of coalescing bubbles;
- the main transport mechanism seems to be the heat pipe effect of evaporation and condensation within the bubble;
- additional convection around the bubbles is observed, which we explain as thermocapillary convection (Marangoni convection).

Similar observations are made in the subcooled $1g$ experiment, here the bubbles remain attached to the surface and the Marangoni convection around the bubbles superimposes the buoyancy convection, which is even strong enough to act against gravity.

7.2.2 Boiling on flat plate

Saturated boiling

Compared to saturated boiling on a wire, the boiling phenomena on a flat plate at very low system pressure of $p/p_c = 0.013$ in R 113 is different. After onset of boiling at a heat flux of 28 kW/m^2 , the first bubble grows slowly within in 1 sec to nearly the size of the heater, see Fig 7. In the film, one can observe that small bubbles are formed in the liquid wedge between the heater and vapor, and immediately coalesce with the larger one. The temperature response of the heater is shown in Fig 8 versus time for μg and $1g$ conditions.



Fig. 7 First growing bubble in R 113 at saturation

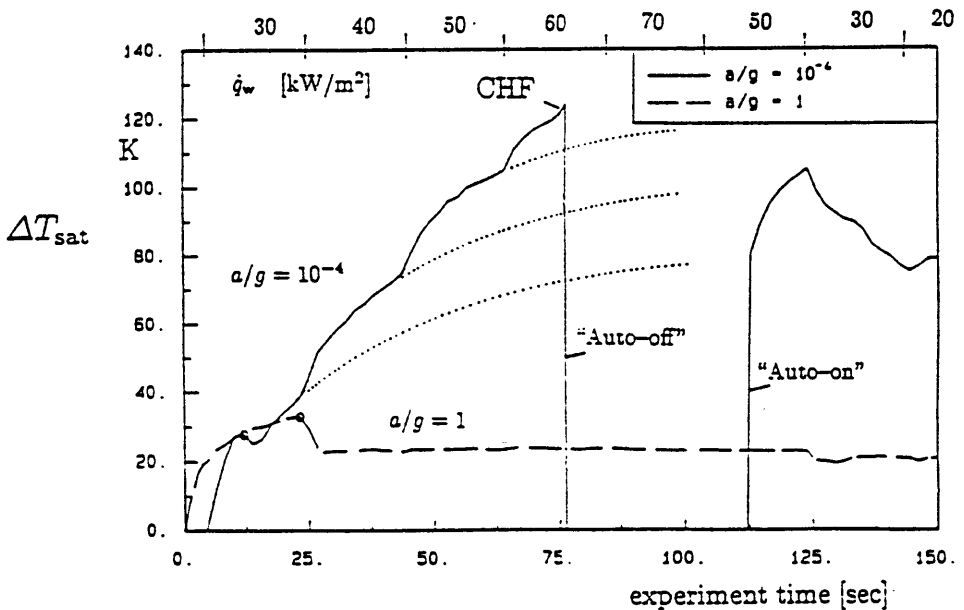


Fig. 8 Temperature response of μg and $1g$ experiment for saturated boiling at low pressure $p/p_c = 0.013$ in R 113

The heat flux is increased in steps of 10 kW/m^2 every 20 seconds, see upper scale. In the μg experiment, the temperature increases after each heat flux step, however, with a decreasing gradient, which indicates a tendency to an asymptotic constant value, which will reach a maximum temperature at about 100 sec experiment time. The second derivative of the temperature increase is

$$\frac{\partial^2 T}{\partial t^2} < 0 \quad (4)$$

which indicates that the final state is stable. It can not be excluded that with a larger heater surface and a longer period of constant heat flux, steady state boiling would have been achieved, however, with the ratio of heat transfer coefficients α/α_1 reduced to 0.3 – 0.2. If we consider that this ratio should be less than 0.01 at $a/g < 10^{-4}$ according to theoretical relations, no agreement can be determined. In microgravity, we observed a transition from nucleate to film boiling. At the 60 kW/m^2 , heat flux step the system runs into a burn-out situation with a strong increase of surface temperature and an increasing gradient. The second derivative is here

$$\frac{\partial^2 T}{\partial t^2} > 0 \quad (5)$$

indicating that the limit of stable nucleate boiling is reached. A further increase of power above the critical heat flux (CHF) would result in an unstable behavior. To avoid that, an automatic control system switches power off. By reducing the power to 50, 30 and 20 kW/m^2 , the surface temperature decreases and it appears that a constant surface temperature on the same level as before can be achieved.

At this low system pressure below CHF, a very large bubble (30 mm in diameter) covers the heater surface. Below the bubble, a dry areas appears, which raises the average heater temperature. The bubble contour is continuously in motion caused by dry out and rewetting and bubble coalescence with smaller bubbles.

Transition from saturated to subcooled boiling:

While the heater was nearly covered by one large bubble, the pressure was increased starting from the saturated situation previously described. Thus, the bulk liquid state was suddenly altered to a subcooling of $\Delta T = 25 \text{ K}$, whereas the heat flux was kept constant at 30 kW/m^2 . Fig 9 demonstrates the immediate thermal stabilization for the μg system.

The vapor of the large bubble was condensed and the system returns to subcooled nucleate boiling after a few seconds. The heater surface temperature is almost equal to the terrestrial reference experiment. Therefore the heat transfer coefficients are the same for μg and earth gravity at this heat flux level.

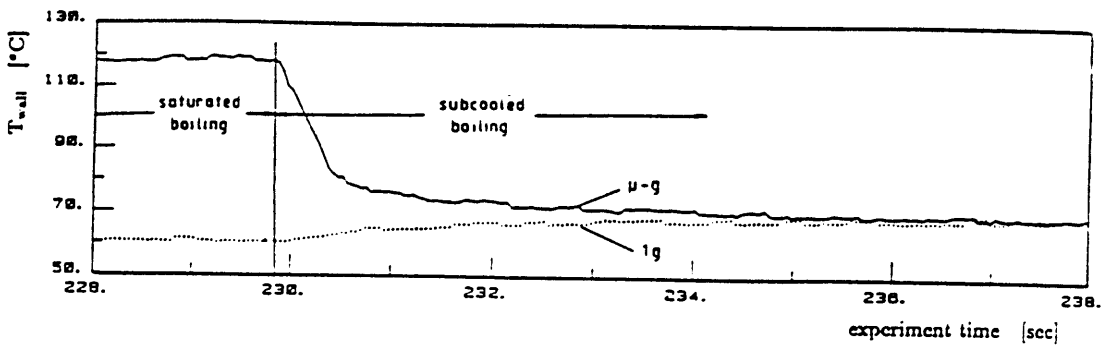


Fig. 9 Transition from saturated to subcooled boiling by pressure increase.

Subcooled boiling

Some experiments of subcooled boiling are performed at various rates of subcooling by variation of pressure. A typical series of pictures of bubble growth is seen in Fig 10. Boiling is first initiated at a single point in the center of the heater surface, and then begins to spread.

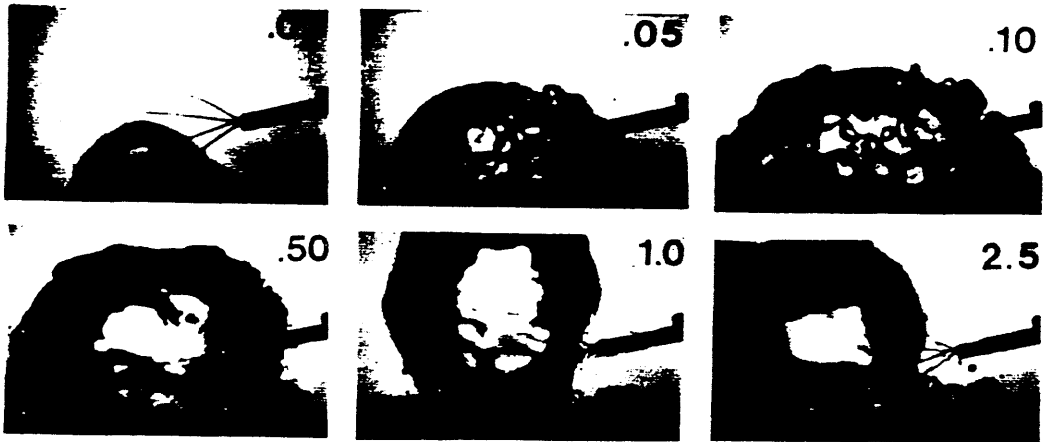


Fig. 10 Development of the first bubble after boiling inception, subcooling $\Delta T = 25 K$

A bubble of semi-spherical shape covered the heater in less than 0.1 seconds. Bubbles formed at the edge of the bubble, are lifted by the growing bubble, that looks pock-marked. This effect may be also due to Marangoni convection. After 1.2 sec the bubble grows large at the base, the smaller bubbles at the base coalesce, or more precisely, feed the larger one. At the top, the bubbles condensate in a very dynamic process. Steady state conditions are reached after about 4 sec.

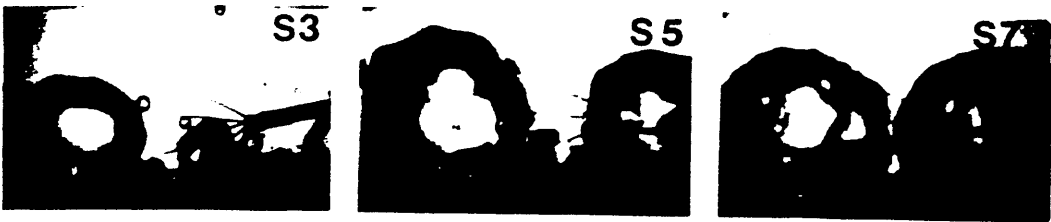


Fig. 11 Pictures of steady state subcooled boiling on a plate for various heat fluxes; 30, 50 and 70 kW/m^2

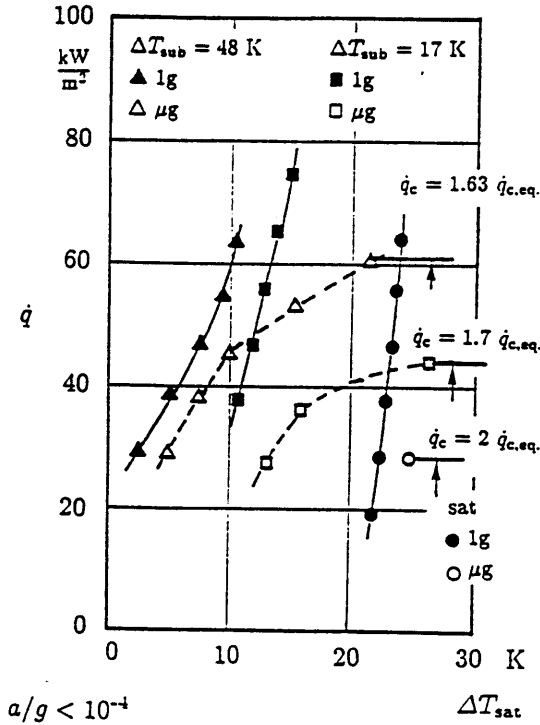


Fig. 12 Boiling curves for the R 113 / flat plate system measured in TEXUS, bulk liquid temperature about 26 °C

At subcooled boiling, we observed that very few bubbles depart from the surface, sometimes they are lifted up and replaced by smaller bubbles growing below. At the same time two larger bubbles are formed, Fig 11, establishing a mass flow through the bubble by evaporation and coalescence at the base and condensation of vapor at the crown. At 50 kW/m^2 the heater temperature slowly increases, however, with a decrea-

sing gradient. A stationary heater temperature might have been achieved, if the period for one heat flux step could be prolonged. This is similar to what we described before at saturated boiling and indicates a transition to CHF. In Fig 12 the boiling curves for saturated and subcooled boiling are plotted. The low gravity curves, in comparison to $1g$, are characterized by higher temperatures and lower heat transfer coefficients.

8. Critical Heat Flux

Theoretical correlations for critical heat flux (CHF) were obtained using the well-known Taylor-Helmholtz instabilities for liquid interfaces. The hydrodynamic instability model by Kutateladse [20] und Zuber [21] for plates predicts the critical heat flux in good agreement with experimental data and is the widely accepted. The relation of Zuber for flat horizontal plates of infinite dimensions with an upward facing surface is written as:

$$\dot{q}_{c,\infty} = 0.131 \cdot h_{l,g} \cdot (\sigma \cdot g \cdot (\rho_l - \rho_g))^{1/4} \sqrt{\frac{\rho_g \cdot \rho_l}{\rho_l + \rho_g}} \quad (6)$$

For heaters of finite dimensions the CHF depends on the geometry as well as its characteristic dimensions. A typical dimension of a hydrostatic instability problem is the Laplace coefficient L , as seen in eq. (2).

Many papers investigate these geometric effects, see the fundamental summary of Lienhard and Dhir [22]. For small tubes and wires with radius R , a dimensionless radius R' , is formed by

$$R' = \frac{R}{L} = R \sqrt{\frac{g(\rho_l - \rho_v)}{\sigma}} \quad (7)$$

and the Zuber relation was extended by Lienhard and Dhir to

$$\dot{q}_{c,R} = 0.94 \cdot \dot{q}_{c,\infty} \cdot R'^{-0.25} \quad (8)$$

valid for $R' < 1$. This relation predicts an increasing CHF for decreasing R' , based on 900 experimental data available at that time, including reduced gravity data. However, a limit was observed at $R' \approx 0.1$; with further decrease of R' , 60 experimental data of CHF decrease as well. Therefore the validity of eq. (8) is assumed between $0,1 < R' < 1$. From eq. (6) the gravity influences for plates and larger tubes can be developed to the critical heat flux relation:

$$\frac{\dot{q}_{c,\infty}}{\dot{q}_{c,\infty,1}} = (a/g)^{1/4} \quad (9)$$

where the index 1 indicates the CHF value at $1g$. For small tubes and wires from equations (6),(7) and (8) the gravity dependence is derived to be:

$$\frac{\dot{q}_{c,R}}{\dot{q}_{c,\infty,1}} \approx (a/g)^{1/8} \quad (10)$$

As discussed before, this relation is valid between $0,1 < R' < 1$. Our experiments at low gravity were conducted to primarily study nucleate boiling and only incidentally CHF, therefore we do not have a full set of experimental data for a proper comparison with the theory. We compared, however, the data received to the equation of Zuber, extended for finite geometries and for wires according to Lienhard and Dhir with the extension from Zuber for subcooled liquids. In this relation the increasing effect of CHF for subcooling is diminished by $(a/g)^{3/4}$.

A properly defined gravity quality is available in the TEXUS experiments with $a/g < 10^{-4}$ and with a wire of a radius 0.1 mm ($R' = 0.001$) we are outside of the valid region of eq. (8) and (10). According to present knowledge, the CHF is much less than the calculated one by eq. (8). Under the given experimental conditions we calculate with Zuber and the correction for small wires from Lienhard and Dhir, the value of 75.6 kW/m^2 for saturated state. However, we have obtained in the experiment 276 kW/m^2 , this is approximately 3.7 times higher than the calculation. In case of subcooled boiling the calculated value for CHF is 135 kW/m^2 , whereas the experimentally obtained one is 450 kW/m^2 , respectively 3.3 times higher than the theory predicts. It is surprising that the CHF data for the wire are more than 3 times higher than predicted, if the relations are extrapolated over the range of their present validity. A decrease of CHF, as found in some experiments, could not be observed for $R' < 0.1$.

In Fig 13 the results for wires are plotted in a similar graph as originally used by Lienhard and Dhir, where the dimensionless radius R' is extended over two decades and the critical heat flux ratio $\dot{q}_{c,R'}/\dot{q}_{c,\infty,1}$ is in a logarithmic scale. The 900 data points which follow the Zuber-Lienhard, Dhir relation are marked as an area and the 60 data points, which miss this relation are also marked. The values obtained in TEXUS for wires at the good low gravity level are about 20 times higher than the predicted values on a flat plate by Zuber and 3.3 to 3.7 times higher than the theory of wires predicts.

The area marked with KC 135 represent about 30 data points from the parabolic flights, which are 1.2 to 2 times higher than the theoretical one on wires. In the parabolic flight experiments the gravity level a/g was alternating between ± 0.03 . We have observed that at a high heat flux the transition to film boiling occurred on the wires if the acceleration was reduced below $|a/g| < 0.005$. The dimensionless radii R' for these experiments are about 10^{-2} .

The calculated critical heat flux for the saturated flat plate experiment in TEXUS is about 14 kW/m^2 , half the value we observed for the onset of boiling. Carefully estimated, we may say, that the experimental CHF is 2 times higher than the calculated one. The same observation is made in the case of subcooled liquids with a factor of 1.7 for $\Delta T_{sub} = 17 \text{ K}$ and 1.63 for $\Delta T_{sub} = 48 \text{ K}$. If we assume, that steady state boiling can be obtained after the asymptotic increase of the average plate temperature according to

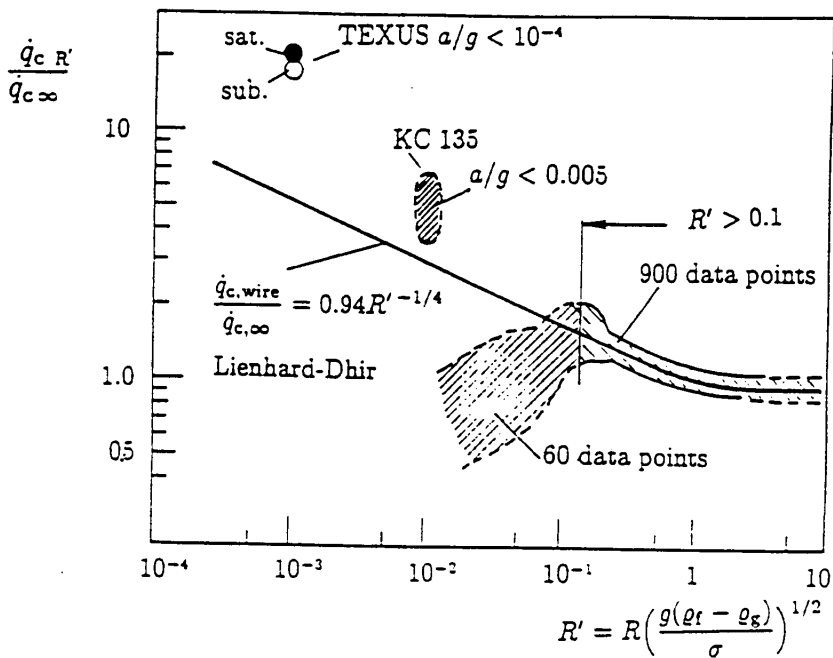


Fig. 13 Critical heat flux for wires similar to a plot of Lienhard and Dhir, extended over two decades in R' and heat flux relation in a logarithmic scale.

Fig 8, the CHF would be even much higher and factors between 3-4 would be obtainable. In Fig 14 the original plot of Siegel [4] is extended in the ordinate in two decades of a/g . On the abscissa the ratio of the experimental CHF to predictions for wires and plates are shown.

The comparison of experimental data with the theory illustrates that the CHF theory based on hydrodynamic instability of the vapor film can not be applied at low gravity. Because buoyancy is not the driving force even in nucleate boiling, surface tension, dry out and rewetting, coalescence and other effects are more dominating. The CHF theory based on the hydrodynamic instability describes the brake down of the vapor film, however in reality, CHF occurs when the vapor film is formed and the nucleate boiling situation is getting unstable by dry out of the liquid below the bubbles. A model considering this situation will be introduced later on.

9. Film Boiling

Nucleate boiling close to the critical heat flux is a situation of great instability, dry out of the heater surface and very difficult to control. By an infinite small increase of the heat flux, the surface is suddenly covered with a vapor film, which yields to a sudden jump of the surface temperature due to the insulation effect of vapor. The transition

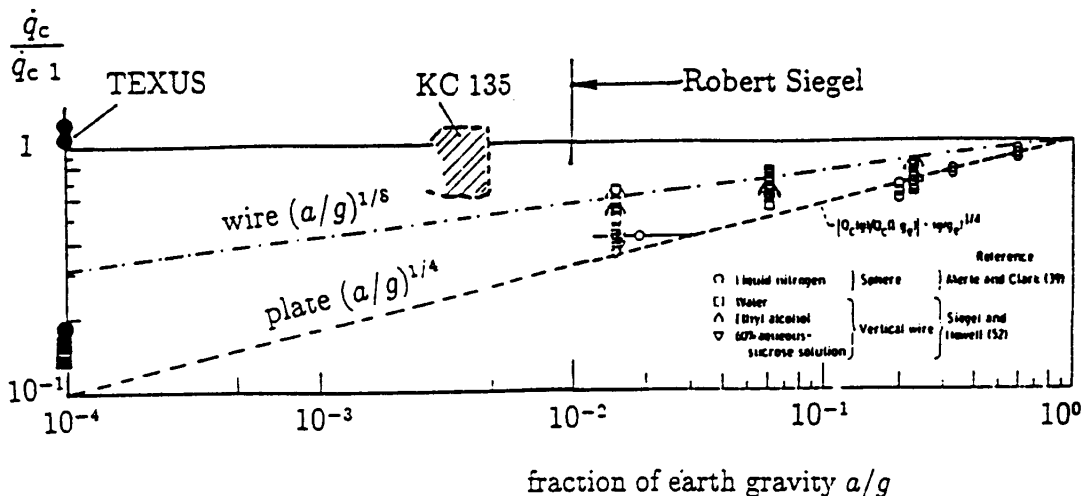


Fig. 14 CHF ratio from Siegel, extended over two decades of a/g

from nucleate to film boiling is shown in a series of pictures, taken from a parabolic flight sequence, and the corresponding records of the acceleration a/g , the temperature difference ΔT_{sat} , and the power, Fig 15.

At the first and following power steps, nucleate boiling occurs with low wire temperature of about $\Delta T_{sat} = 10 K$. At a heat flux of $300 kW/m^2$ the system change to film boiling with an increase of ΔT_{sat} to $300 K$. Now small a/g -variations change the heater temperature, but film boiling is still maintained during $1.8g$ and $1g$ periods. The photos show the different behavior of the closed vapor film. It is formed by surface tension into a chain of large and small bubbles with a distance of about the Laplace length. The small bubbles pump the vapor toward the larger bubbles by the pressure difference between them and peristaltic motion. The vapor hose is very sensitive to disturbances of the a/g -level, which can be seen in the temperature record. The vapor hose is no more symmetrically around the wire, which influences the heat transfer between the wire and the liquid phase.

Several correlations exist for film boiling, all based on the film theory of Nusselt for condensation. One of the earliest relations is from Bromley [23], which can be analyzed for its gravity dependence of the heat transfer coefficients according to eq. (5) with the exponent $n = 0.25$.

The film boiling data of Merte and Clark [24] on spheres in liquid nitrogen at low gravity down to $a/g = 0.017$, and Freon 113 data at high gravity up to $a/g = 10$, are in agreement with the correlation of Frederking and Clark [25], which represents the gravity dependence with $n = 1/3$. For smaller cylinders and wires, Pitschmann [26] extended the relation from Bromley including the influence of radiation and the Smoluchowsky effect for low density gases. Its influence on gravity is given by $n = 0.16$.

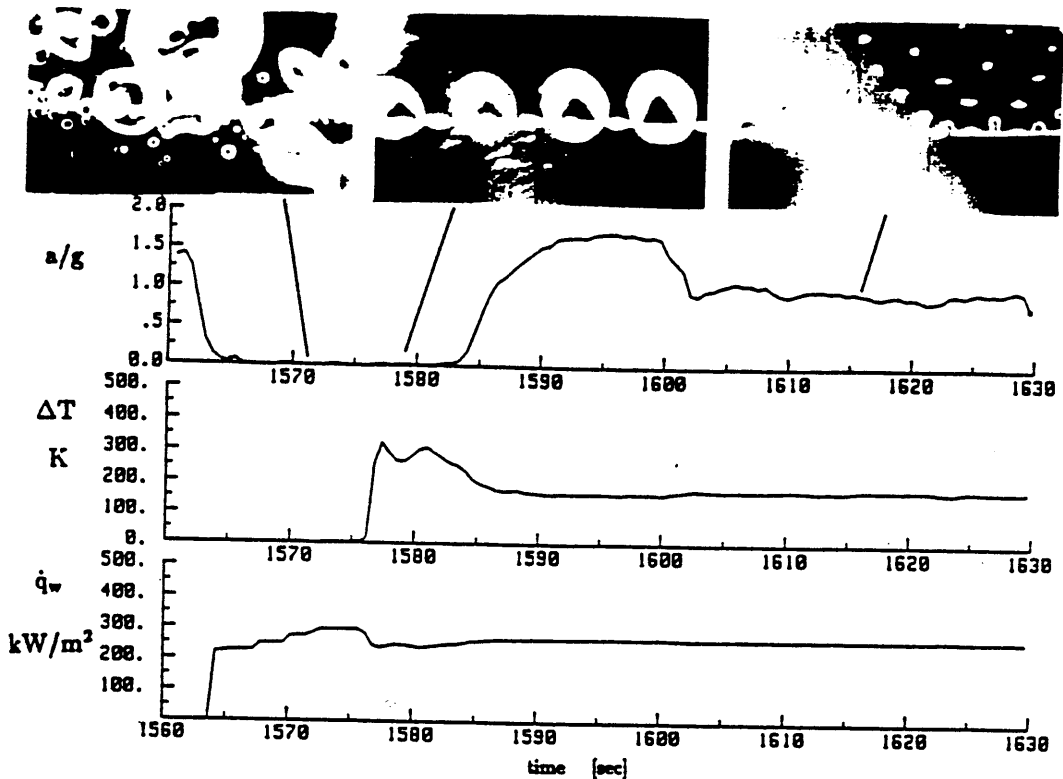


Fig. 15 Sequence of a parabola, with transition to film boiling

The correlations of Pitschmann, Bromley and Frederking and Clark are in agreement with our data on R 12 at saturation, with wires having 0.05 mm and 0.2 mm diameters; Pitschmann is on the upper and Frederking is at the lower limit of the scatter band, see Fig 16. However, it seems that at $a/g = 5 \cdot 10^{-2}$, the heat transfer coefficient is nearly independent of further gravity reduction. This result is confirmed by data obtained during film boiling in TEXUS experiments with $\alpha/\alpha_1 = 0.48$ and 0.38. This is explained by the dominating effect of surface tension as seen in Fig 15. A chain of large and small bubbles are formed around the wire, and vapor is pumped from the small bubbles into the large bubbles due to the higher pressure, whereby the smaller bubbles continuously change size. In TEXUS it was observed that a very large bubble of approx. 20 mm in diameter was formed, and a chain of small bubbles with decreasing diameters at increasing distance from the larger one pump the vapor into the large bubble at a high frequency. We therefore assume that correlations derived on the basis of boundary-layer theory may no longer be applied for $a/g < 5 \cdot 10^{-2}$; surface tension, radiation and axial flow of the vapor within the bubble chain is the mechanism dominating the heat transport. However, we also found that small variations in gravity influence the bubble

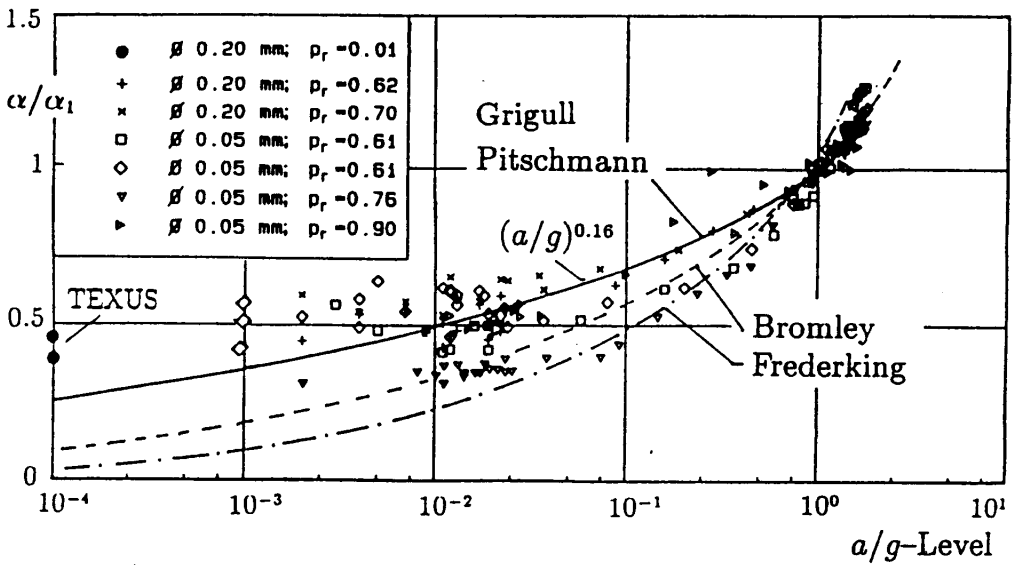


Fig. 16 Measured film boiling data and corresponding correlations

chain. It is no longer arranged symmetrically around the wire as under very low gravity conditions.

The evaluation of subcooled data shows a more distinct gravity dependence with $\alpha/\alpha_1 = (a/g)^{0.25}$. The bubbles around the wire are not as spherical than at saturated state, they are deformed and Marangoni convection around them can be observed.

10. The mechanisms of boiling in the various modes of heat transfer

10.1 Nucleate boiling

Our experimental finding in boiling microgravity research is that nucleate pool boiling heat transfer is more or less nearly independent of the gravity level over a large pressure range between $0.1 < p/p_c < 0.7$. Only at very low and high pressures the influence of gravity is remarkable, however much less than predicted by theoretical and empirical correlations. At low pressures and high heat fluxes, the bubbles grow to large size and thus dry areas below them are formed and yield to an increase of the observed average temperature of the heater due to an insulation effect. At high pressures, the lower surface tension seems to be the limiting factor. However, boiling seems to be nearly independent of buoyancy and the departure size of the bubbles over a wide range of fluid states, which is in contradiction to most of the present conceptions of boiling.

The question, however, remains: what are the forces and the mechanisms to drive the nucleate boiling heat transfer at reduced gravity, if the dominating buoyancy force is changed to lower negligible values? Thus we can draw the following conclusions, that

the boiling process must be divided into a primary mechanism and several secondary mechanisms:

- The primary mechanism is the formation and the growth of the bubbles themselves by evaporation at their base in the superheated liquid boundary layer. Most important for the heat transfer is the wedge at the three phase interface, solid-liquid-vapor on the baseline of the bubbles. In this corner the evaporation rate will be very high. This evaporation is not determined by gravity, but only by the temperature of the heater. We could observe that in the liquid-solid wedge below large bubbles continuously new bubbles are formed, which then coalesce and feed the larger ones.
- The secondary process, just as important, is the transport of the latent heat and the superheated liquid of the boundary layer away from the surface, which occurs at earth gravity by buoyancy. At low gravity, however, it is replaced by other mechanisms. Here we have to decide between saturated and subcooled fluid states.

10.2 The micro-wedge model

The primary mechanisms are most important for the heat transfer in boiling, which take place in the small wedge between the solid-liquid, solid-vapor and liquid-vapor interfaces, we call it „micro-wedge“, see Fig 16. In this region the heat transfer rate determined by the evaporation rate is very high and independent from gravity. It is determined by the heater temperature, the heat transport through the thin liquid film in the wedge between the heater and the bubble interface, the evaporation at the interface and the liquid flow to the interface due to capillary forces.

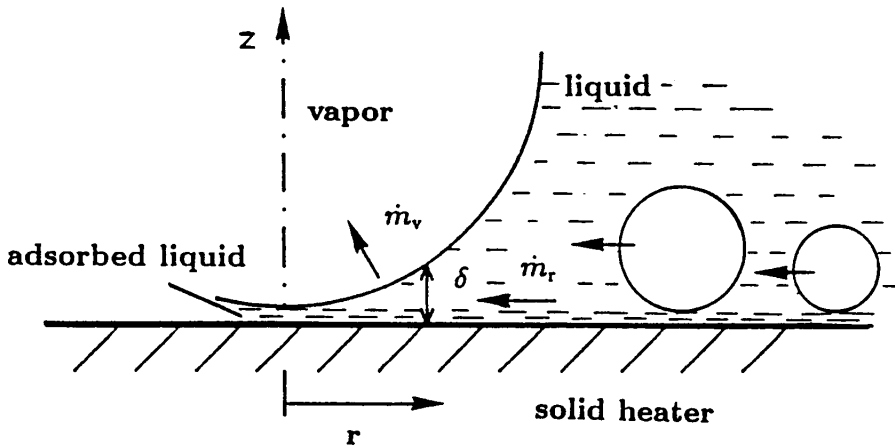


Fig. 17 Micro-wedge modell of nucleate boiling. Nucleate boiling is stable for $\dot{m}_v = \dot{m}_r$ and unstable for $\dot{m}_v > \dot{m}_r$ (CHF, transition to film boiling)

In a simplified manner, we can treat this model similar to a evaporating liquid film. In this thin film, pure heat conduction is assumed, thus the heat flux density \dot{q} in the z -direction can be written as:

$$\dot{q}(r) = \frac{\lambda}{\delta(r)} (T_w - T_p) = \dot{m}_v(r) \cdot \Delta h \quad (11)$$

where λ is the thermal conductivity of the liquid and $\delta(r)$ the thickness of the liquid film. T_w is the surface temperature of the heater, which is even a function of r , and T_p is the temperature on the liquid side at the interface, which is depending on $\delta(r)$ and the evaporation rate. In a first approach, we assume $T_p \approx T_{sat}$, the saturation temperature corresponding to the system pressure.

The evaporation rate \dot{m}_B for a single bubble is expressed by the kinetic theory of evaporation integrated over the active area of the bubble:

$$\dot{m}_B = \int_{(B)} 2\pi r \cdot \dot{m}_v dr = \int_{(B)} 2\pi r \cdot \beta_v \sqrt{\frac{k}{2\pi m^*}} \left(\frac{p_p}{\sqrt{T_p}} - \frac{p_v}{\sqrt{T_v}} \right) dr \quad (12)$$

where β_v is the evaporation coefficient, k the Boltzmann constant and m^* the mass of the molecule. p stands for the pressure and T for the temperature, both having indices p for the interface of the liquid and v for the vapor side. Using eq.(12), the heat flux rate per bubble is expressed with the evaporation enthalpy Δh as:

$$\dot{Q}_B = \dot{m}_B \cdot \Delta h \quad (13)$$

The flow in direction towards the interface is caused by capillary forces due to non-equilibrium conditions at the interface, which result from the strong evaporation and a deviation of curvature from the equilibrium value. With the assumption that the flow in the wedge is in steady state, slow and parallel to the wall, the momentum equation is simplified to :

$$\frac{\partial p_f}{\partial z} = -\eta \frac{\partial^2 u_r}{\partial z^2} \quad (14)$$

with η as the dynamic viscosity, u_r the velocity in r -direction and p_f the pressure of the liquid. $\partial p_f / \partial z$ is due to the change of capillary pressure according to the change of curvature. With eq.(11) – (14), the handling of the micro-wedge model is only indicated. In reality, an unsteady flow and bubble growth have to be considered additionally. During the first rapid growth of a bubble the liquid flow is not developed, moreover the liquid is pushed aside by the expansion of the bubble. However, in case of larger bubbles under microgravity the flow in the wedge is evident and can be observed via the migration of smaller bubbles. The numerical integration of the differential equations yield to the heat transport of one bubble. The overall heat transfer takes the number

of active nucleate site into account, which is depending on the superheat of the liquid in the boundary layer. In subcooled liquids, additional heat transport mechanisms are the thermocapillary flow from the base to the cap of the bubble and the heat pipe effect by evaporation and condensation inside the bubble.

10.3. Secondary mechanisms

Secondary mechanisms are responsible for the heat and mass transport from the heater surface to the bulk liquid by departing bubbles carrying away latent heat, by wake flow following the bubbles and by convection. In pool boiling under earth gravity, the buoyancy is the driving force for these processes. In microgravity various effects are observed mainly caused by surface tension, like vertical and horizontal bubble coalescence and displacement of larger bubbles by smaller ones. If bubbles coalesce, liquid is set into motion and by its inertia and momentum the bubbles are lifted from the surface. More details about these effects are described in recent publications [27].

10.4 Critical heat flux

If nucleate boiling can be maintained even at high heat flux values at low gravity conditions, the hydrodynamic theory of liquid film instability can no longer be applied for CHF. As mentioned before, the description of the physics, which leads to CHF, seems not to be an adequate description. A theory of CHF has to describe the formation of the vapor film from nucleate boiling first, and the second step can be the hydrodynamic instability of the film, which leads to steady state film boiling. With the micro-wedge model, we can easily understand the development to CHF. At high heat flux, the absorbed liquid film will evaporate with increasing wall temperature. The evaporation mass flow gets higher than the liquid mass flow towards the interface, caused by the smaller capillary forces. The dynamic wetting angle increases as well as the dry area below the bubble. According to Fig 16, we can state:

stable nucleate boiling is maintained as long as: $\dot{m}_v = \dot{m}_r$

unstable transition to film boiling via CHF occurs if: $\dot{m}_v > \dot{m}_r$

The unstable situation may occur simultaneously on neighboring bubbles and spreads rapidly over the entire heater surface forming a closed vapor film. As a consequence, the average heater temperature is increasing rapidly and the nucleate boiling regime changes to film boiling via critical heat flux.

10.5 Film boiling

It was previously discussed that even film boiling can be stabilized and maintained as long as the vapor production is large enough to fulfill the Kelvin Helmholtz stability. At present no experience exists, how long such a situation can be maintained. This also

appears to apply to plates and tubes. At wires, a chain of bubbles with large and small diameters is formed around the wire by surface tension. The vapor produced is pumped by contracting and expanding of smaller bubbles in a peristaltic motion. Vapor flow and the increasing heater temperature intensify the heat transfer by radiation, maintaining the heat transfer coefficient lower than at $1g$, however, nearly constant at $\alpha_0/\alpha_1 = 0.5$ for $a/g < 10^{-2}$. The existing theories based on Nusselt film theories be extrapolated to this acceleration value.

11. Conclusions

In this report, we have presented a short survey of the latest development in pool boiling heat transfer under microgravity conditions. Our project is part of the German microgravity research program and also part of the German Japanese cooperation. It is of interest to note that buoyancy acting on the bubbles and buoyancy convection are not the mechanisms controlling the heat transfer in boiling. The buoyancy is replaced by other powerful mechanisms caused by surface tension and capillary forces. The primary mechanism, which determines the heat transfer nearly independent of gravity, is caused by the heat transfer in the wedge between the heater surface and the bubble. Important is the evaporation at the interface and the liquid mass flow to the interface caused by capillary forces in this small wedge. We have presented here a micro-wedge model, which explains the insensitivity of boiling heat transfer of the actual value of gravity, and explains the critical heat flux as an instability at the interface line solid, liquid, vapor on the base of the bubble and the transition to film boiling. However, there are still many open questions to understand the physics behind the boiling process completely and to improve our knowledge, which is based on 60 years of research. Microgravity offers the unique opportunity to eliminate the strong buoyancy effects, and to look deeper into the process itself. However, this research is limited by the flight opportunities and therefore the continuation of international cooperation as it exists with a Japanese research ground at ETL in Tsukuba should be intensified.

Acknowledgments

Our research project has been sponsored by the Bundesminister für Forschung und Technologie, BMFT, represented by DLR/DARA. We also gratefully thank all teams involved in the project for their kind assistance.

References

- [1] Nukiyama, S. (1934):
The Maximum Values of the Heat Q Transmitted from Metall to Boiling Water Under Atmospheric Pressure; Trans. JSME, Vol. 37, p. 367, reprinted in Int. J. Heat Mass Transfer, Vol. 9, pp 1419-1433
- [2] Dhir, V.K. (1990):
Nucleate and Transition Boiling Heat Transfer Under Pool Boiling and External Flow Conditions; Proc. 9th Int. Heat Transfer Conf., Jerusalem 1990, Hemisphere Pub., New York
- [3] Fritz, W. (1935):
Berechnungen des Maximalvolumens von Dampfblasen; Phys. Z. 36, pp. 379 - 384
- [4] Siegel, R. (1967):
Effects of Reduced Gravity on Heat Transfer; Advances in Heat Transfer, Vol. 4, Academic Press, New York/ London, pp. 143-228
- [5] Clark, J.A. (1968):
Gravic and Agravic Effects in Cryogenic Heat Transfer; Advances in Cryogenic Heat Transfer 87, Vol. 64, pp. 93 - 102
- [6] Verkin, B.I.; Kirichenko, Y.A. (1976):
Heat Transfer under Reduced Gravity Conditions; Acta Astronautica, Vol. 3, Pergamon Press, pp. 471-480
- [7] Merte, H. jr. (1990):
Low Gravity Fluid Dynamics and Transport Phenomena; in: Progress in Astronautics and Aeronautics, Vol 130, edited by J.N. Koster and R.L. Sani
- [8] Weinzierl, A.; Straub, J. (1982):
Subcooled Pool Boiling in Microgravity Environment; Proc. 7th Int. Heat Transfer Conference, Munich (1982), Vol.4, pp. 21-27
- [9] Zell, M.; Weinzierl, A.; Straub, J. (1984):
Nucleate Pool Boiling in Subcooled Liquid under Microgravity - Results of TEXUS Experimental Investigations; Proc. 5th European Symposium on Material Sciences under Microgravity - Schloß Elmau, (1984), ESA SP-222, pp. 327-333
- [10] Weinzierl, A. (1984):
Untersuchung des Wärmeübergangs und seiner Transportmechanismen bei Siedevorgängen unter Schwerelosigkeit; Dissertation TU München

- [11] Weinzierl, A.; Straub, J.; Zell, M. (1986):
Spacelab Nutzung: Untersuchung des Wärmeübergangs und seiner Transportmechanismen bei Siedevorgängen unter Schwerelosigkeit; BMFT Forschungsbericht W86-021
- [12] Straub, J.; Zell, M. (1988):
Messung der Siedekurven unter Schwerelosigkeit; Abschlußbericht des FV 01 QV 8501 BMFT
- [13] Zell, M.; Straub, J., Vogel, B. (1989):
Pool Boiling Under Microgravity; J. PhysicoChemical Hydrodynamics, Vol. 11, No. 5/6, pp. 813-823
- [14] Straub, J.; Zell, M. and Vogel, B. (1990):
Pool Boiling in a Reduced Gravity Field; Proc. 9th Int. Heat Transfer Conf., Jerusalem 1990
- [15] Zell, M. (1991):
Untersuchung des Siedevorgangs unter reduzierter Schwerkraft; Ph.D. thesis, Technische Universität München
- [16] Straub, J., Zell, M. and Vogel, B. (1992):
Boiling under Microgravity Conditions; Proc. First European Symposium Fluids in Space, Ajaccio, France, Nov. 18-22, 1991, ESA SP-353, pp. 269-297
- [17] Vogel, B. and Straub, J. (1992):
Single Bubble Experiments in Pool Boiling - Results from TEXUS 26; Proc. Eighth European Symposium on Materials and Fluid Sciences in Microgravity, Bruxelles, Belgium, April 12-16, ESA-SP 333, Bd. 2, pp. 879-886
- [18] Ervin, J.S.; Merte, H. jr.; Keller, R.B. and Kirk, K. (1992):
Transient Pool Boiling in Microgravity; Int. J. Heat Mass Transfer, Vol. 35, No. 3, pp. 659-74
- [19] Oka, T.; Abe, Y.; Tanaka, K.; Mori, Y.H. and Nagashima, A. (1992):
Observational Study of Pool Boiling under Microgravity; JSME Int. Journal, Series 2, Vol. 35, No. 2, pp. 280-286
- [20] Kutateladse, J.J. (1963):
Fundamentals of Heat Transfer; Edward Arnold Ltd., translated from Russian
- [21] Zuber, N. (1959):
Hydrodynamic Aspect of Boiling Heat Transfer; AECU - 4439, USA
- [22] Lienhard, J.H.; Dhir, V.K. (1973):
The Extended Hydrodynamic Theory of the Peak and Minimum Pool Boiling Heat Fluxes; NASA CR 2270

- [23] Bromley, LeRoy A. (1950):
Heat Transfer in Stable Film Boiling; Chem. Eng. Prog. Ser. 46, pp. 221-227
- [24] Merte, H. jr.; Clark, J. A. (1963):
Boiling Heat Transfer to a Cryogenic Fluid in Both Low and High Gravity Fields;
Proc. XIth Congress of Refrigeration, Munich (1963), pp. 347-355
- [25] Frederking, T.H.K.; Clark, J.A. (1963):
Natural Convection Film Boiling on a Sphere; Advances in Cryogenic Engineering, Vol. 8, p. 501, New York
- [26] Pitschmann, P. (1968):
Wärmeübergang von elektrisch beheizten horizontalen Drähten an Flüssigkeiten bei Sättigung und natürlicher Konvektion; BMWF-Forschungsbericht K68-53
- [27] Straub, J. (1993):
The Role of Surface Tension for Heat Transfer in Absence of Gravity; Proc. 3rd Int. Conf. of Heat Transfer, Thermodynamics, Honolulu, Hawaii, Nov 1993